Reversal effects of low-dose imatinib compared with sunitinib on monocrotaline-induced pulmonary and right ventricular remodeling in rats

Zi Ping Leong [a,b], Ayumi Okida [b], Masahi Higuchi [a,c], Yoshiaki Yamano [a,c], Yoshiaki Hikasa [a,b,*]

[a] The United Graduate School of Veterinary Science, Yamaguchi University, 1677-1, Yoshida, Yamaguchi 753-8515, Japan

[b] Laboratory of Veterinary Internal Medicine, Joint Department of Veterinary Medicine, Faculty of Agriculture, Tottori University, Tottori 680-8550, Japan

[c] Laboratory of Veterinary Biochemistry, Joint Department of Veterinary Medicine, Faculty of Agriculture, Tottori University, Tottori 680-8550, Japan

*Corresponding author. E-mail address: hikasa@muses.tottori-u.ac.jp (Y. Hikasa)

Abstract

High-dose imatinib reverses cardiopulmonary remodeling but adverse effects limit its clinical use. Efficacy of the multi-kinase inhibitor sunitinib remains questionable. We compared anti-remodeling effects of imatinib with sunitinib on monocrotaline-induced right ventricular (RV) hypertrophy and pulmonary arterial remodeling in rats, focusing on a lower dose. Fourteen days after monocrotaline injection, oral gavage of imatinib (5, 15, or 50 mg/kg), sunitinib (0.3, 1, 3, or 10 mg/kg), or water for 14 days was started. RV hypertrophy and brain natriuretic peptide mRNA levels were significantly and dose-dependently reduced, much greater in imatinib- than sunitinib-treated groups. Imatinib normalized muscularization of 20 - 50 μm intra-acinar pulmonary arteries more significantly than sunitinib. At transcript levels, sunitinib significantly upregulated pulmonary nestin, and downregulated platelet-derived growth factor receptor beta (PDGFR-β), fibroblast growth factor receptor 1, vascular endothelial growth factor receptor-2 and vascular endothelial growth factor (VEGF)-A, but not Raf-1 proto-oncogene serine/threonine kinase mRNAs. Sunitinib also suppressed VEGF-A, but not phosphorylated extra-cellular-signal-related kinase (ERK)-1/2 protein expression. The sole PDGFR-β antagonism of imatinib resulted in significant Raf-1 mRNA and phosphorylated ERK-1/2 protein downregulation, suggesting that the equivocal reversal effect of sunitinib may be due to its VEGF signaling inhibition in the lung. Imatinib's greater dose-dependent reversal on cardiopulmonary remodeling may make a low dose suitable for PAH treatment.

Keywords: Cardiopulmonary remodeling, imatinib, sunitinib, pulmonary arterial hypertension.

1. Introduction

Pulmonary arterial hypertension (PAH) entails small pulmonary artery proliferation and remodeling, resulting in a rise in mean pulmonary pressure ≥ 25 mmHg at rest [19] and eventually right-sided heart failure [25, 36]. With a poor prognosis of reported survival rates of 58%, 41% and 24% in patients receiving a single therapy after 1, 2 and 3 years, respectively [33], dual or triple combination therapy targeting any of the three main mechanistic pathways (endothelin, nitric oxide, and prostacyclin) for PAH treatment improved the survival outcome [17-20, 33, 48-49]. However, long-term prognosis of PAH treatment remains poor [13, 39].

Role of mitogen-activated protein kinase (MAPK) pathway in pathogenesis of PAH has been documented [31, 46], which involves upstream signaling from various receptor tyrosine kinases (TK) such as platelet-derived growth factor receptor beta (PDGFR-β) [4, 46, 55], fibroblast growth factor receptor (FGFR)-1 [5, 53, 57], endothelial growth factor receptor (EGFR) [9], and C-Kit receptor [14, 40]. Imatinib, a TK inhibitor, reverses pulmonary and myocardial remodeling in the rodent models [8, 12, 46] and significantly improves right ventricular (RV) functions in the PAH patients [21, 47, 50] and the Phase III Imatinib in Pulmonary Arterial Hypertension, A Randomized, Efficacy Study (IMPRES) [24]. However, an extension of the IMPRES revealed disappointing outcomes and adverse effects in imatinib-treated PAH patients [16]. In 2013, Novartis withdrew imatinib for PAH treatment.

To develop new therapies for PAH, sparing of the receptor TK pathways from the current treatment algorithm is our concern. Many experimental and clinical PAH studies did not investigate whether low-dose TK inhibitors are effective without producing associated deleterious effects. Our study on PAH dogs showed that a low-dose imatinib therapy for 30 days reduced pulmonary arterial pressure and improved cardiac function and hemodynamics [3]. Similarly, a clinical study using low-dose imatinib in PAH patients showed improved diffusion capacity of the lung for carbon monoxide (DLCO) and varying hemodynamic responses [23]. However, these clinical studies did not investigate anti-remodeling effects of the low-dose therapy on cardiopulmonary remodeling assessed at tissue and molecular levels. Thus, we revised the study to investigate several imatinib and sunitinib doses, emphasizing on the lowest anti-remodeling dose possible. We also aimed to compare the effects of

imatinib with sunitinib on pulmonary and RV remodeling to determine whether imatinib yields a greater anti-remodeling effect than sunitinib.

2. Methods

2.1. Monocrotaline-induced pulmonary arterial remodeling

Eight-week-old, male, Wistar-Imamichi rats were purchased from the Institute for Animal Reproduction, Ibaraki, Japan, and randomized into control, placebo, and treatment groups. Under isoflurane anesthesia, monocrotaline (MCT, Sigma-Aldrich, China) was subcutaneously injected at 60 mg/kg body weight to the placebo and treatment rats to induce pulmonary arterial remodeling. Physiological saline solution was injected to the control rats. Fourteen days after the injection, oral gavage was started once daily, such that the treatment rats received imatinib mesylate [Glivec, Novartis: 5 (Ima-5), 15 (Ima-15), or 50 (Ima-50) mg/kg per day] or sunitinib malate [SUTENT®, Pfizer: 0.1 (Suni-0.1), 1 (Suni-1), 3 (Suni-3), or 10 (Suni-10) mg/kg per day], whereas the control and placebo rats received water. The oral gavage was continued for 14 days after which the rats were euthanized for tissue sampling. All protocols were approved by the Institutional Animal Care and Use Committee of the Tottori University.

2.2. Assessment of RV hypertrophy

The right ventricular (RV) tissue was separated from the left ventricle and septum (LV + S). RV and (LV + S) wet weights were determined to obtain the RV hypertrophy (RVH) index given by the formula: RV / (LV + S).

2.3. Pulmonary artery histology and pulmonary arterial muscularization assessment

The left lung lobe caudal to the bronchus was excised and fixed in 10% formalin neutral buffer solution. Lung tissues were outsourced to Sapporo General Pathology Laboratory Co. Ltd., Japan, for histology and slide preparation, as well as staining with elastic van Gieson (EVG) and double staining of EVG and alpha-smooth muscle actin (α-SMA) antibody. Under light microscopy (400 × magnification), intra-acinar artery (IA) images were captured by an Olympus Digital Camera DP21. Approximately 300 IAs (20 – 50 μm in diameter) were identified and counted as fully muscularized

(FMIA), partially muscular (PMIA), and non-muscular (NMIA) to obtain the proportion of each artery type and calculate muscularization percentage (Fig. 1A). For FMIAs between 20 – 50 μm and 51 – 100 μm in diameter, external diameter (*d*) and medial wall thickness (MWT) were measured using Image J software. In addition, medial MWT ratio given by MWT normalized to diameter ($2 \times MWT / d$), lumen diameter ($d - 2 \times MWT$), and lumen area [$3.142 \times (d / 2)^2$] of the FMIAs were also determined.

2.4. ELISA measurement of serum N-terminal pro-brain natriuretic peptide (NT-proBNP) levels

Blood was sampled via cardiac puncture into plain blood tubes. Serum was obtained after centrifuging the clotted blood at 3500 rpm for 5 min (Kubota 4000, Japan). Enzyme-linked immunosorbent assay (ELISA) for rat serum NT-proBNP was performed using a commercial kit (Cloud-Clone Corp., Wuhan, China), in accordance to the manufacturer's protocol. Absorbance was read at 450 nm by an iMark^{TM} microplate reader (BIORAD, Japan). A standard curve was constructed to give readings of serum NT-proBNP levels (ng/mL).

2.5. RNA extraction, reverse transcription, and semi-quantitative fast real-time polymerase chain reaction

The RV tissue and the right caudal lung lobe were stored in RNA*later*® solution (Ambion™, Austin, TX, USA). Total RNA was isolated from tissue homogenates using TRIzol® Reagent (Ambion™, USA), in accordance to the manufacturer's specifications. First-strand cDNA was synthesized from 2 μg of the total RNA using the Superscript® III First-Strand Synthesis System (Invitrogen, USA). Primers were designed and ordered from the Japan Food Assessment and Management Center (FASMAC) (Fig. 1B). Relative quantifications of the target mRNAs of PDGFR-β, FGFR-1, VGFR-2, VEGF-A, nestin, Raf-1, b-type natriuretic peptide (BNP), and the house-keeping gene glyceraldehyde 3-phosphate dehydrogenase (GAPDH) were determined by Applied Biosystems 7500 Fast Real-Time PCR System using SYBR® Fast qPCR Mix (Takara Bio Inc., Shiga, Japan) containing 400 nM of each forward and reverse primers for rats.

2.6. Western blotting assay

Lung tissues were homogenized in T-PER® Tissue Protein Extraction Reagent (Thermo Fisher Scientific, USA) containing 1% protease and phosphatase inhibitors (Thermo Fisher Scientific, USA).

Total protein concentrations were determined by Bradford assay (Quick Start™ Bradford Protein Assay Kit, Bio-Rad, USA). Lysates containing 50 μg total soluble protein were resolved on 4 – 15 % SDS-polyacrylamide gels (Mini-PROTEAN® TGX™ Precast Protein Gels, Bio-Rad, USA) and transferred to polyvinylidene difluoride membranes. The membranes were blocked in Tris-buffered saline (EzTBS, Atto, Tokyo, Japan) containing 1% bovine serum albumin and then probed with a specific primary antibody of either anti-phospho-ERK 1/2 (Cell Signaling Technology, Inc., USA), anti-ERK 1/2 (C9) (Santa Cruz Biotechnology Inc., Santa Cruz, CA, USA), anti-VEGF-A (Abcam, Cambridge, UK) or anti-β-actin (Santa Cruz Biotechnology Inc., Santa Cruz, CA, USA), followed by a secondary antibody conjugated to horseradish peroxidase. Chemiluminescence was visualized using Bio-Rad Universal Hood II and quantified by Image Lab Software 6.0 (Bio-Rad Laboratories).

2.7. Statistical analyses

All data are expressed as mean ± standard error of mean (SEM). Data were analyzed for statistical differences using the StatMate3 analysis software (ATMS, Tokyo, Japan). Inter-group differences for normally distributed data were analyzed using one-way analysis of variance, followed by a least significant difference post-hoc test for multiple comparisons. Differences between two independent groups were analyzed using student T-test for normally distributed data or Mann–Whitney U test for non-normally distributed data. The relationship between treatment effects and dosages was analyzed using simple linear regression and Pearson correlation test. $P < 0.05$ was considered to be significant.

3. Results

3.1. Effect of imatinib and sunitinib on RVH and cardiac remodeling biomarkers

The placebo developed a severe RVH with a significant increase in the RV / [LV + S] ratio (0.54 ± 0.03) compared with the control (0.22 ± 0.01) (Fig. 2A). Treatment with ima-15 and ima-50 significantly reversed the RVH, yielding a stronger dose-dependency (R^2: 0.16; $P < 0.05$) than sunitinib (R^2: 0.09; $P < 0.05$) (Fig. 2B). None of the sunitinib-treated groups significantly reduced the RVH, although a weak reversal tendency was observed.

BNP mRNA was markedly increased in the placebo (0.54 ± 0.03) and lowest in the control group (0.07 ± 0.01) (Fig. 2C). All imatinib treatment groups showed reduced BNP mRNA expression compared with the placebo, of which significant reductions were observed in ima-15 (0.36 ± 0.08) and ima-50 (0.31 ± 0.05) groups. Sunitinib-treated rats also showed a slight reduction in BNP mRNA expression. Only the suni-10 group had a significant reduction (0.38 ± 0.06) compared with the placebo.

In tandem with the mRNA results, serum NT-proBNP levels were the highest in the placebo (0.68 ± 0.22 ng/mL) (Fig. 2D). Compared with the placebo, treatment with imatinib or sunitinib reduced serum NT-proBNP levels in rats, although none reached statistical significance.

3.2. Effect of imatinib and sunitinib on pulmonary remodeling

3.2.1. Muscularization of 20 – 50 μm IAs

Control rats had the highest NMIA percentage (39.08 ± 1.91 %). The MCT injection induced remodeling in the rat pulmonary vasculature indicated by the lowest NMIA percentage in the placebo (8.33 ± 1.14 %) (Fig. 3A). Compared with the placebo, imatinib-treated groups showed an approximately two-fold increase in the NMIA percentage (16.67 ± 1.93 % for ima-5; 17.22 ± 2.22 % for ima-15; 21.50 ± 2.18 % for ima-50) and these increases achieved a statistical significance. Except the suni-3 group (12.53 ± 0.87 %), the other sunitinib-treated groups significantly increased the NMIA percentage (12.69 ± 1.48 % for suni-0.3; 15.86 ± 1.94 % for suni-1; 17.15 ± 1.34 % for suni-10). Imatinib exhibited a stronger dose-dependency than sunitinib (R^2: 0.29; $P < 0.05$ and R^2: 0.14, respectively).

Conversely, the FMIA percentage was the lowest in the control rats (15.14 ± 1.73 %) and the highest in the placebo rats (42.39 ± 2.06 %) due to proliferation of the arterial smooth muscle cells. Treatment with imatinib significantly and dose-dependently reversed muscularization degree in the pulmonary vasculature (R^2: 0.17; $P < 0.05$) (Fig. 3B). However, muscularization reduction was not statistically significant in sunitinib-treated rats (R^2: 0.01; $P < 0.05$).

3.2.2. Medial hypertrophy and lumen area of 20 – 50 μm FMIAs

We investigated degree of smooth muscle proliferation of the FMIAs by examining the MWT ratio and the lumen area of the IAs. The MWT ratio was the highest in the placebo (49.37 ± 1.26 %) and the

lowest in the control (34.95 ± 1.23 %) (Fig. 3C). Although all imatinib and sunitinib groups showed decreased MWT ratios, the reduction was only significant in the groups of ima-15 (45.79 ± 1.17 %), ima-50 (45.38 ± 1.08 %), and suni-1 (46.00 ± 0.87 %).

The placebo had the smallest lumen area (229.10 ± 8.69 μm²), which differed significantly from that of the control (392.87 ± 15.60 μm²) (Fig. 3D). Ima-15 (296.70 ± 10.77 μm²), ima-50 (298.51 ± 26.94 μm²) and suni-1 (281.92 ± 14.55 μm²) groups had significantly larger lumen areas than the placebo. Only imatinib dose-dependently normalized the lumen area of the IAs (R^2: 0.22; $P < 0.05$ for imatinib and R^2: 0.002 for sunitinib).

3.2.3. Medial hypertrophy and lumen area of 51 – 100 μm FMIAs

The MCT injection also significantly induced medial wall thickening of the 51 – 100 μm IAs in the placebo (53.58 ± 1.86 %) compared with that of the control (38.89 ± 1.86 %) (Fig. 4A). Imatinib and sunitinib treatments significantly reduced the MWT but only the imatinib groups produced a noticeable dose-dependency (R^2: 0.22; $P < 0.05$ for imatinib; R^2: 0.01 for sunitinib).

The lumen area of the 51–100 μm FMIAs was the smallest in the placebo (899.50 ± 68.10 μm²), which differed significantly compared to that of the control group (1514.44 ± 87.05 μm²) and all the treatment groups (Fig. 4B). Increases in lumen area in the imatinib groups were dose-dependently compared to those in the sunitinib groups (R^2: 0.15; $P < 0.05$ for imatinib; R^2: 0.02 for sunitinib).

3.3. Effect of imatinib and sunitinib on relative expression of PDGFR-β and FGFR-1 mRNA in the lungs

The MCT injection significantly upregulated the PDGFR-β mRNA expression in the placebo (0.088 ± 0.013) compared with that in the control (0.032 ± 0.005) (Fig. 5A), suggesting a role of PDGFR-β in the vascular remodeling process. Imatinib and sunitinib treatments reduced PDGFR-β mRNA expression, with significant reductions observed in ima-15 (0.048 ± 0.007), ima-50 (0.051 ± 0.008), suni-1 (0.023 ± 0.008), suni-3 (0.016 ± 0.005), and suni-10 (0.023 ± 0.002) groups.

The marked upregulation of FGFR-1 mRNA in the placebo group (0.056 ± 0.008) also confirmed the role of FGFR-1 in vascular remodeling (Fig. 5B). None of the imatinib groups showed significant downregulation of FGFR-1 mRNA expression. Conversely, suni-1 (0.024 ± 0.006), suni-3 (0.022 ± 0.003), and suni-10 (0.024 ± 0.002) groups showed significant downregulation of FGFR-1 mRNA

expression compared with that in the placebo. Suni-3 and suni-10 groups had significantly lower mRNA expression than the control (0.037 ± 0.003).

3.4. Effect of imatinib and sunitinib on VEGF signaling pathway in the lungs

3.4.1. VEGFR-2 mRNA expression

VEGFR-2 mRNA expression was comparable between control (0.292 ± 0.035), placebo (0.287 ± 0.021), and all imatinib groups (Fig. 6A). However, VEGFR-2 mRNA expression was significantly downregulated in suni-1 (0.176 ± 0.023), suni-3 (0.173 ± 0.022), and suni-10 (0.136 ± 0.014) groups compared with those of control and placebo. VEGFR-2 was also dose-dependently inhibited by sunitinib (R^2: 0.28; $P < 0.05$).

3.4.2. VEGF-A mRNA and protein expression

Since VEGF-A supplies the VEGF signaling pathway, we further investigated the mRNA (Fig. 6B) and protein (Fig. 6C) expression. Surprisingly, the control had insignificantly higher levels of mRNA (0.074 ± 0.016) and protein (0.519 ± 0.063) than the placebo (0.052 ± 0.005 for mRNA; 0.489 ± 0.010 for protein). Compared with the above groups, the mRNA and protein levels were significantly lower in suni-3 (0.026 ± 0.004 for mRNA; 0.286 ± 0.022 for protein) and suni-10 (0.025 ± 0.003 for mRNA; 0.281 ± 0.010 for protein) groups. Suni-1 also significantly inhibited the protein expression (0.317 ± 0.008). In the ima-15 group, a significant reduction of the mRNA (0.036 ± 0.005) but not the protein (0.469 ± 0.056) was seen compared with that of the placebo. Further, we observed a stronger dose-dependent VEGF-A inhibition in sunitinib (R^2: 0.24, $P < 0.05$ for mRNA; R^2: 0.36, $P < 0.05$ for protein) than imatinib (R^2: 0.09 for mRNA; R^2: 0.02 for protein).

3.5. Effect of imatinib and sunitinib on relative VEGFR-2 mRNA expression in the RV

VEGFR-2 mRNA expression of RV tissues did not significantly differ among the groups (Fig. 6D). The placebo showed a lower VEGFR-2 mRNA expression level than the control, whereas suni-1, suni-3 and suni-10 groups had a lower mRNA level than the placebo.

3.6. Effect of imatinib and sunitinib on MAPK signaling pathway in the lungs

3.6.1. Raf-1 mRNA expression

The placebo exhibited significant upregulation of Raf-1 mRNA expression (0.15 ± 0.02) compared with control (0.07 ± 0.01) (Fig. 7A). Ima-15 (0.10 ± 0.01) and ima-50 (0.08 ± 0.01) significantly inhibited the Raf-1 mRNA expression. The inhibition was not significant in all sunitinib groups except for suni-10 (0.06 ± 0.01).

3.6.2. Phosphorylated ERK-1/2 protein expression

Phosphorylated ERK-1/2 protein expression was noticeably increased in the placebo (3.26 ± 0.38), suni-3 (2.12 ± 0.43) and suni-1 (2.37 ± 0.16) groups, compared with that in the control group (0.39 ± 0.12) (Fig. 7B). Ima-15 (0.48 ± 0.09), ima-50 (0.19 ± 0.10), and suni-10 groups (0.06 ± 0.02) significantly suppressed the protein phosphorylation to a level comparable with that of the control group.

3.7. Effect of imatinib and sunitinib on relative nestin mRNA expression in the lungs

To explain reversal differences between imatinib and sunitinib on pulmonary remodeling, we examined nestin mRNA expression in all groups (Fig. 8A). The placebo had nestin mRNA levels statistically comparable with the control 28 days after the MCT injection (0.047 ± 0.013 for placebo versus 0.034 ± 0.006 for control). However, ima-5 (0.068 ± 0.012), suni-0.3 (0.062 ± 0.011), suni-1 (0.062 ± 0.011), and suni-3 (0.068 ± 0.013) groups had significantly upregulated nestin mRNA levels. There were no significant changes in expression levels between control and placebo groups even 42 days after the injection (0.025 ± 0.006 for placebo versus 0.055 ± 0.015 for control) (Fig. 8B).

4. Discussion

This study provides a new perspective on the effects of imatinib by investigating its dose-dependency to show that a lower dose (15 mg/kg) is equally effective compared with a high dose (50 mg/kg) in the reversal of monocrotaline-induced pulmonary and cardiac remodeling in rats. We also show that imatinib exerts stronger anti-remodeling actions than sunitinib perhaps attributable to on-going proliferation of pulmonary arteries due to VEGF signaling disruption by sunitinib.

Twenty-eight days post-MCT injection, the muscularized small intra-acinar arteries markedly increased at the expense of the non-muscularized arteries in rat lungs. This is accompanied by a severe medial hypertrophy, leading to narrowing of the lumen area of the arteries as highlighted by EVG and/or α-SMA staining, indicating the occurrence of a vascular remodeling process. We also observed

significant RVH, indicative of myocardial remodeling after the MCT injection. The above results are consistent with those of previous studies that used MCT as a toxic model of PAH [31, 34, 46, 56].

We confirmed the previously reported data of elevated PDGFR-β [4, 46, 56] and FGFR-1 transcript levels [5, 53, 57], and decreased VEGFR-2 and the VEGF-A levels [2, 15, 41, 44, 54] thus affirming the pathogenic role of PDGFR-β and FGFR-1 in MCT-induced pulmonary remodeling. In terms of kinase selectivity, imatinib targets 9 kinases whereas sunitinib possesses a greater spectrum of activity which targets 30 receptor tyrosine kinases [30]. In our study, sunitinib potently blocked PDGFR-β, FGFR-1, VEGFR-2, and VEGF-A mRNAs, while imatinib only significantly inhibited PDGFR-β mRNA in rat lungs. Given that these receptor tyrosine kinases and their respective growth factors activate the MAPK signaling pathway [29], and Raf-1 kinase is the entry point to this downstream signaling pathway [10], we expected a greater downregulation of the MAPK signaling pathway in the sunitinib-treated groups. However, significant down-regulation of Raf-1 mRNA and phosphorylated ERK-1/2 protein expressions was only seen in the highest dose of sunitinib treatment group. As for the imatinib treatment groups, ima-15 and ima-50 significantly blocked the MAPK pathway. This suggests that sunitinib's multiple kinase inhibition did not translate into a greater inhibition of the MAPK downstream signaling pathway in MCT-induced cardiopulmonary remodeling compared with imatinib of a narrower kinase target.

For myocardial remodeling, imatinib reversed RVH at 15 and 50 mg/kg and elicited a higher dose-dependency than sunitinib. However, despite the weak reversal observed, none of the sunitinib groups produced a significant RVH reversal, which disagrees with the findings of Kojonazarov et al [32]. Our data agree with those of Hung et al [26] and Vitalia et al [51], that mice subjected to hypoxia developed a more severe form of RVH after receiving Sugen (SU5416), an anti-VEGF therapy than those subjected to hypoxia alone. As for the cardiac biomarker, the 15 and 50 mg/kg imatinib groups significantly down-regulated the BNP mRNAs, but only rats on a 10 mg/kg dose in the sunitinib groups produced a significant decrease in the BNP mRNA expression. Because VEGFR-2 mRNA levels of RV did not differ significantly among all groups, the lack of a significant reversal by sunitinib might be related to the remodeling process in the pulmonary vasculature.

Imatinib was reported to reverse pulmonary remodeling at a dose of 50 and 100 mg/kg/day [46]. However, the anti-remodeling effect of lower doses remains uncertain, although studies which evaluated clinical effectiveness of low-dose imatinib on PAH have been conducted on a small sample of human patients [23] and dogs [3], respectively. Our present study shows that imatinib at 5, 15 and 15 mg/kg significantly reduced the FMIAs and increased the NMIAs of 20 – 50 μm in diameter, consistent with the clinical observations in the above studies. Conversely, sunitinib did not significantly normalize medial hypertrophy nor lumen area of the FMIAs in rats. These findings support the earlier statement of an equivocal RVH improvement in sunitinib groups, which may be attributable to a lack of pulmonary remodeling reversal.

Further, we examined nestin mRNA expression in lungs of the MCT-injected rats. Nestin, an intermediate filament protein recently discovered as a more specific angiogenesis marker for small arteries than CD31, CD34, and von Willebrand factor [35, 43], is highly expressed during angiogenesis following a vascular insult and in various forms of neoplasm [1, 27, 38, 43] as well as in pulmonary remodeling [7]. Saboor et al recently showed that nestin plays a role in the proliferation of vascular smooth muscle cells and provides a diagnostic tool for pulmonary hypertension [45]. However, to the best of our knowledge, no studies have reported on nestin expression in rat lungs after treatment with imatinib or sunitinib. We demonstrated that the sunitinib treatment groups (0.3, 1 and 3 mg/kg) significantly upregulated nestin mRNA expression compared with that in imatinib, control, and placebo groups. Twenty-eight days after the MCT injection, the placebo group did not show increased nestin mRNA expression, which agrees well with findings of Saboor et al [45], which stated that nestin expression is upregulated only during the initial phase of pulmonary remodeling. To further clarify this finding, we showed that the placebo rat lungs did not upregulate nestin mRNA expression even after 42 days after the MCT injection, indicating that the pulmonary vasculature had established a quiescent state. Therefore, upregulated nestin mRNA expression and increased pulmonary muscularization, further evident by the lack of significant MAPK pathway inhibition in the sunitinib groups compared with that in the imatinib groups, led us to believe that sunitinib but not imatinib treatment induced on-

going proliferation of the smooth muscle cells in the small intra-acinar arteries, in a phenomenon known as “escape angiogenesis” [6, 42] and/or non-canonical angiogenesis [11].

Since VEGF overexpression protects against hypoxic and MCT-induced PAH [52], one possible reason to explain continued proliferation of smooth muscle cells induced by sunitinib is inhibition of the VEGF signaling pathway. Despite the severe pulmonary remodeling in the placebo group, an apparent overexpression of VEGFR-2 and VEGF-A mRNAs as well as VEGF-A protein was not observed, consistent with the results by Arcot et al [2], Nadeau et al [41], and Farkas et al [15], which also reported decreased VEGF and/or VEGFR mRNA expression levels in PAH rats induced with monocrotaline and/or chronic hypoxia. While imatinib did not affect the VEGF signaling pathway, sunitinib significantly and dose-dependently downregulated VEGFR-2 and VEGF-A levels. Since Sugen (SU5416) was used for its VEGFR inhibiting actions to further enhance the angioproliferative PAH in mice subjected to hypoxia [26, 51] or mice were treated with a repeated immunization of ovalbumin [37], we believe that the lack of effectiveness in reversing the vascular remodeling in sunitinib groups is attributable to its potent inhibition of the VEGF signaling pathway.

In a study which evaluated the long-term safety and efficacy of imatinib in human PAH [16], the authors concluded that imatinib resulted in severe adverse effects, significant side effects, and a high discontinuation rate that limited imatinib use in PAH treatment. The study utilized a starting dose of 200 mg once daily and up-titrated to 400 mg once daily (which is equivalent to a rat dose of 50 mg/kg in our study and the neoplastic dose indicated for gastrointestinal stromal carcinoma and chronic myeloid leukemia treatment in humans) [22]. In a study by Hatano et al [23], five PAH patients who received a low-dose imatinib at 100 mg/day (equivalent to a rat dose of 12.5 mg/kg) for 12 weeks, showed improved DLCO and hemodynamic parameters as indicated by either a decreased mean pulmonary arterial pressure, a decreased pulmonary venous resistance, or an increased cardiac index. When the treatment was extended to 24 weeks, only three patients showed sustained favorable effects. Further, our previous PAH study in dogs also showed that treatment with 3 mg/kg of imatinib, a dose equivalent to a 1/3 dose of the 10 mg/kg used to treat canine malignancies [28], improved clinical scores and echocardiographic outcomes in dogs [3]. Taken together, the above clinical observations could be

explained by the potent anti-remodeling of low-dose imatinib (15 mg/kg). Therefore, we believe that low-dose of imatinib has the advantage of reducing side effects, yet is effective to reverse pulmonary vascular remodeling and right ventricular hypertrophy that characterize PAH.

5. Conclusion

Imatinib elicited dose-dependent anti-remodeling actions, and a dose as low as 15 mg/kg, significantly inhibited the MAPK signaling pathway responsible for pulmonary vascular remodeling and RVH in MCT-injected rats. Imatinib is more effective than sunitinib in reversing MCT-induced cardiopulmonary remodeling in rats, through inhibition of PDGFR-β while sparing VEGF inhibition in the lungs. Therefore, low-dose imatinib therapy may provide an option for treatment of pulmonary arterial hypertension and concomitant RVH.

Acknowledgments

We thank Dr. Takehito Morita and Ms. Sae Sanematsu for their valuable technical assistance.

Disclosures

This study was supported in part by the Grant-in-Aid for challenging Exploratory Research from the Japan Society for the Promotion of Science (no. 25660240; to Y. Hikasa) and the 2016 Tottori University President Discretion Grant (to Y. Hikasa).

References

[1] Aihara M, Sugawara K, Torii S, Hosaka M, Kurihara H, Saito N, et al. Angiogenic endothelium-specific nestin expression is enhanced by the first intron of the nestin gene. *Lab Invest* 2004; **84**: 1581–1592.

[2] Arcot SS, Lipke DW, Gillespie MN, Olson JW. Alterations of growth factor transcripts in rat lungs during development of monocrotaline-induced pulmonary hypertension. *Biochem Pharma* 1993; **46**: 1086–1091.

[3] Arita S, Arita N, Hikasa Y. Therapeutic effect of low-dose imatinib on pulmonary arterial hypertension in dogs. *Can Vet J* 2013; **54**: 255–261.

[4] Balasubramaniam V, Le Cras TD, Ivy DD, Grover TR, Kinsella JP, Abman SH. Role of platelet-derived growth factor in vascular remodeling during pulmonary hypertension in the ovine fetus. *Am J Physiol Lung Cell Mol Physiol* 2003; **284**: L826–L833.

[5] Benisty JI, McLaughlin VV, Landzberg MJ, Rich JD, Newburger JW, Rich S, et al. Elevated basic fibroblast growth factor levels in patients with pulmonary arterial hypertension. *Chest* 2004; **126**: 1255–1261.

[6] Carmeliete PK. Keystone Conference of Pulmonary Hypertension. September 10-15, 2012. Monterey, California USA. [Personal communication]

[7] Chabot A, Meus MA, Naud P, Hertig V, Dupuis J, Villeneuve L, et al. Nestin is a marker of lung remodeling secondary to myocardial infarction and type I diabetes in the rat. *J Cell Physio* 2015; **230**: 170–179.

[8] Chaumais MC, Perros F, Dorfmuller P, Traclet J, Cohen-Kaminsky S, Simonneau G, et al. Nilotinib and imatinib therapy in experimental pulmonary hypertension. *Am J Respir Crit Care Med* 2012; **185**: A3419; doi: http://dx.doi.org/10.1164/ajrccm-conference.2012.185.1_MeetingAbstracts.A3419.

[9] Dahal BK, Cornitescu T, Tretyn A, Pullamsetti SS, Kosanovic D, Dumitrascu R, et al. Role of epidermal growth factor inhibition in experimental pulmonary hypertension. *Am J Respir Crit Care Med* 2009; **181**: 158–167.

[10] Dhillon AS, Kolch W. Untying the regulation of the Raf-1 kinase. Arch Biochem Biophys 2002; **404**: 3–9.

[11] Domigan CK, Ziyad S, Iruela-Arispe ML. Canonical and non-canonical VEGF pathways: New developments in biology and signal transduction. *Arterioscler Thromb Vasc Biol* 2015; **35**: 30–39.

[12] Duggan N, Bonneau O, Hussey M, Quinn DA, Manley P, Walker C, et al. Comparison of effects of imatinib and nilotinib in a rodent model of pulmonary arterial hypertension. *Am J Respir Crit*

Care Med 2010; **181**: A6304, doi: http://dx.doi.org/10.1164/ajrccm-conference.2010.181.1_MeetingAbstracts.A6304.

[13] Farber HW, Miller DP, Poms AD, Badesch DB, Frost AE, Muros-Le Rouzic E, et al. Five-year outcomes of patients enrolled in the REVEAL registry. *Chest* 2015; **148**:1043–1054.

[14] Farha S, Dweik R, Rahaghi F, Benza R, Hassoun P, Frantz R, et al. Imatinib in pulmonary arterial hypertension: C-Kit inhibition. *Pulm Circ* 2014; **4**: 452–455.

[15] Farkas L, Farkas D, Ask K, Möller A, Gauldie J, Margetts P, et al. VEGF ameliorates pulmonary hypertension through inhibition of endothelial apoptosis in experimental lung fibrosis in rats. *J Clin Invest* 2009; **119**: 1298–1311.

[16] Frost AE, Barst RJ, Hoeper MM, Chang HJ, Frantz RP, Fukumoto Y. Long term safety and efficacy of imatinib in pulmonary arterial hypertension. *J Heart Lung Transpl* 2015; **34**: 1366–1375.

[17] Galie N, Corris PA, Frost A, Girgis RE, Granton J, Jing ZC, et al. Updated treatment algorithm of pulmonary arterial hypertension. *J Am Coll Cardiol* 2003; **62**: D60–D72.

[18] Galie N, Hoeper MM, Humbert M, Torbicki A, Vachiery J-L, Barbera JA, et al. Guidelines for the diagnosis and treatment of pulmonary hypertension. *Eur Respir J* 2009; **34:** 1219–1263.

[19] Galie N, Hoeper MM, Humbert M, Torbicki A, Vachiery JL, Barbera JA, et al. Guidelines for the diagnosis and treatment of pulmonary hypertension: the Task Force for the Diagnosis and Treatment of Pulmonary Hypertension of the European Society of Cardiology (ESC) and the European Respiratory Society (ERS), endorsed by the International Society of Heart and Lung Transplantation (ISHLT). *Eur Heart J* 2009; **30**: 2493–2537.

[20] Ghofrani HA, Humbert M. The role of combination therapy in managing pulmonary arterial hypertension. *Eur Respir Rev* 2014; **23**: 469–475.

[21] Ghofrani HA, Morrell NW, Hoeper MM, Olschewski H, Peacock AJ, Barst RJ, et al. Imatinib in pulmonary arterial hypertension patients with inadequate response to established therapy. *Am J Respir Crit Care Med* 2010; **182**: 1171–1177.

[22] Guilhot F. Indications for imatinib mesylate therapy and clinical management. *Oncologist* 2004; **9**: 271–281.

[23] Hatano M, Yao A, Shiga T, Kinugawa K, Hirata Y, Nagai R. Imatinib mesylate has the potential to exert its efficacy by down-regulating the plasma concentration of platelet-derived growth factor in patients with pulmonary arterial hypertension. *Int Heart J* 2010; **51**: 272–276.

[24] Hoeper MM, Barst RJ, Bourge RC, Feldman J, Frost AE, Galie N, et al. Imatinib mesylate as add-on therapy for pulmonary arterial hypertension: Results of the randomized IMPRES study. *Circulation* 2013; **127**: 1128–1138.

[25] Humbert M. Update in pulmonary hypertension 2008. *Am J Respir Crit Care Med* 2009; 179: 650–656.

[26] Hung VT, Emoto N, Vignon-Zellweger N, Nakayama K, Yagi K, Suzuki Y, et al. Inhibition of vascular endothelial growth factor under hypoxia causes severe, human-like pulmonary arterial hypertension in mice: Potential roles of interleukn-6 and endothelin. *Life Sci* 2014; **118**: 313–328.

[27] Ishiwata T, Teduka K, Yamamoto T, Kawahara K, Matsuda Y, Naito Z. Neuroepithelial stem cell marker nestin regulates the migration, invasion and growth of human gliomas. *Oncol Rep* 2011; **26**: 91–99.

[28] Isotani M, Ishida N, Tominaga M, Tamura K, Yagihara H, Ochi S, et al. Effect of tyrosine kinase inhibition by imatinib mesylate on mast cell tumors in dogs. *J Vet Intern Med* 2008; **22**: 985–988.

[29] Katz M, Amit I, Yarden Y. Regulation of MAPKs by growth factors and receptor tyrosine kinases. Arch Biochem Biophys 2007; **1773**: 1161-1176.

[30] Kitagawa D, Yokota K, Gouda M, Narumi Y, Ohmoto H, Nishiwaki E, et al. Activity-based kinase profiling of approved tyrosine kinase inhibitors. *Genes Cells* 2013; **18**: 110–122.

[31] Klein M, Schermuly RT, Ellinghaus P, Milting H, Riedl B, Nikolova S, et al. Combined tyrosine and serine/threonine kinase inhibition by sorafenib prevents progression of experimental pulmonary hypertension and myocardial remodeling. *Circulation* 2008; **118**: 2081–2090.

[32] Kojonazarov B, Sydykov A, Pullamsetti SS, Luitel H, Dahal BK, Kosanovic D, et al. Effects of multikinase inhibitors on pressure overloaded-induced right ventricular remodeling. *Int J Cardiol* 2013; **167**: 2630–2637.

[33] Kylhammar D, Persson L, Hesselstrand R, Radegran G. Prognosis and response to first-line single and combination therapy in pulmonary arterial hypertension. *Scand Cardiovasc J* 2014; **48**: 223–233.

[34] Lalich JL, Johnson WD, Raczniak TJ, Shumaker RC. Fibrin thrombosis in monocrotaline pyrrole-induced cor pulmonale in rats. *Arch Pathol Lab Med* 1977; **101**: 69–73.

[35] Matsuda Y, Hagio M, Ishiwata T. Nestin: A novel angiogenesis marker and possible target for tumor angiogenesis. *World J Gastroenterol* 2013; **19**: 42–48.

[36] McLaughlin VV. Looking to the future: a new decade of pulmonary arterial hypertension therapy. *Eur Respir Rev* 2011: **20**: 262–269.

[37] Mizuno S, Farkas L, Alhussaini A, Farkas D, Gomez-Arroyo L, Kraskauskas D, et al. Severe pulmonary arterial hypertension induced by SU5416 and ovalbumin immunization. *Am J Respir Cell Mol* 2012; **47**: 679–687.

[38] Mokry J, Cízkova D, Filip S, Ehrmann J, Osterreicher J, Kolar Z, et al. Nestin expression by newly formed human blood vessels. *Stem Cells Dev* 2004; **13**: 658–664.

[39] Montani D, Chaumais M-C, Guignabert C, Gunther S, Girerd B, Jais X, et al. Targeted therapies in pulmonary arterial hypertension. *Pharmacol Ther* 2014; **141**: 172–191.

[40] Montani D, Perros F, Gambaryan N, Girerd B, Dorfmuller P, Price LC, et al. C-kit-positive cells accumulate in remodeled vessels of idiopathic pulmonary arterial hypertension. *Am J Respir Crit Care Med* 2011; **184**: 116–123.

[41] Nadeau S, Baribeau J, Janvier A, Perreault T. Changes in expression of vascular endothelial growth factor and its receptors in neonatal hypoxia-induced pulmonary hypertension. *Pediatr Res* 2005; **58**: 199–205.

[42] Nicolls M, Mizuno S, Taraseviciene-Stewart L, Farkas L, Drake JI, Husseini AA, et al. New models of pulmonary hypertension based on VEGF receptor blockade-induced endothelial cell apoptosis. *Pulm Circ* 2012; **2**: 434–442.

[43] Oikawa H, Hayashi K, Maesawa C, Masuda T, Sobue K. Expression profiles of nestin in vascular smooth muscle cells in vivo and in vitro. *Exp Cell Res* 2010; **316**: 940–950.

[44] Partovian C, Adnot S, Eddahibi S, Teiger E, Levame M, Dreyfus P, et al. Heart and lung VEGF mRNA expression in rats with monocrotaline- or hypoxia-induced pulmonary hypertension. *Am J Physiol Cell Physiol* 1998; **44**: H1948–H1956.

[45] Saboor F, Reckmann AN, Tomczyk CU, Peters DM, Weissmann N, Kaschtanow A, et al. Nestin-expressing vascular wall cells drive development of pulmonary hypertension. *Eur Respir J* 2016; **47**: 876–888.

[46] Schermuly RT, Dony E, Ghofrani HA, Pullamsetti S, Savai R, Roth M, et al. Reversal of experimental pulmonary hypertension by PDGF inhibition. *J Clin Invest* 2005; **115**: 2811–2821.

[47] Shah AM, Campbell P, Rocha GQ, Peacock A, Barst JB, Quinn D, et al. Effect of imatinib as add-on therapy on echocardiographic measures of right ventricular function in patients with significant pulmonary arterial hypertension. *Eur Heart J* 2015; **36**: 623–632.

[48] Sitbon O, Jais X, Savale L, Cottin V, Bergot E, Macari EA, et al. Upfront triple combination therapy in pulmonary arterial hypertension: a pilot study. *Eur Respir J* 2014; **43**: 1691–1697.

[49] Sitbon O, Sattler C, Bertoletti L, Savale L, Cottin V, Jaïs X, et al. Initial dual oral combination therapy in pulmonary arterial hypertension. *Eur Respir J* 2016; **47**: 1727–1736.

[50] Souza R, Sitbon O, Parent F, Simonneau G, Humbert M. Long term imatinib treatment in pulmonary arterial hypertension. *Thorax* 2006; **61**: 736.

[51] Vitalia SH, Hansmanna G, Rose C, Fernandez-Gonzalez A, Scheid A, Mitsialis SA, et al. The Sugen 5416/hypoxia mouse model of pulmonary hypertension revisited: Long-term follow-up. *Pulmonary Circulation* 2014; **4**: 619–629.

[52] Voelkel NF, Vandivier RW, Tuder RM. Vascular endothelial growth factor in the lung. *Am J Physiol Lung Cell Mol Physiol* 2006; **290**: L209–L221.

[53] Xin X, Johnson AD, Scott-Burden T, Engler D, Casscells W. The predominant form of fibroblast growth factor receptor expressed by proliferating human arterial smooth muscle cells in culture is type I. *Biochem Biophys Res Commun* 1994; **204**: 557–564.

[54] Yamamoto A, Takahashi H, Kojima Y, Tsuda Y, Morio Y, Muramatsu M, et al. Downregulation of angiopoietin-1 and Tie in chronic hypoxic pulmonary hypertension. *Respiration* 2008; **75**: 328–338.

[55] Yu Y, Sweeney M, Zhang S, Platoshyn O, Landsberg J, Rothman A, et al. PDGF stimulates pulmonary vascular smooth muscle cell proliferation by upregulating TRPC6 expression. *Am J Physiol Lung Cell Mol Physiol* 2003; **284**: C316–C330.

[56] Zhang B, Niu W, Xu D, Li Y, Liu M, Wang Y, et al. Oxymatrine prevents hypoxia and monocrotaline-induced pulmonary hypertension in rats. *Free Radic Biol Med* 2014; **69**: 198–207.

[57] Zheng Y, Ma H, Hu E, Huang Z, Cheng X, Xiong C. Inhibition of FGFR signaling with PD173074 ameliorates monocrotaline-induced pulmonary arterial hypertension and rescues BMPR-II expression. *J Cardiovasc Pharmacol* 2015; **66**: 504–514.

A

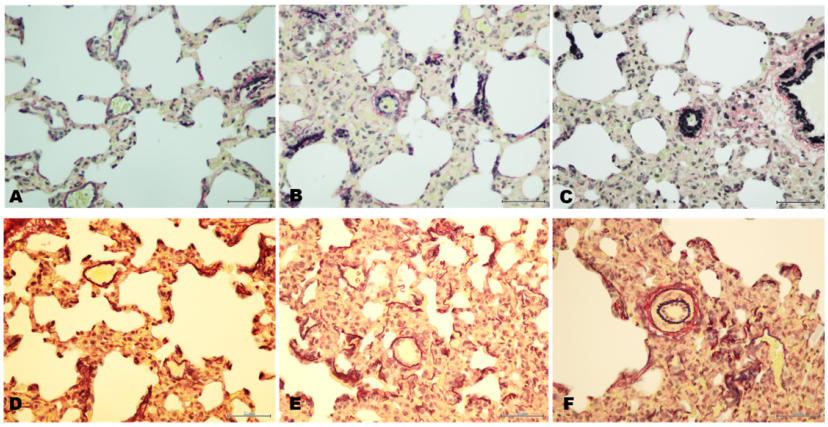

B

Gene	Accession Number	Symbol	Forward Primer	Reverse Primer
B-type natriuretic peptide	NM_031545.1	BNP	CAGAAGCTGCTGGAGCTGATA	GGCGCTGTCTTGAGACCTAA
Fibroblast growth factor receptor type 1	NM_024146.1	FGFR-1	GCAGCGATACCACCTACTTCT	CCTACGGTTTGGTTTGGTGTT
Vascular endothelial growth factor receptor 2	NM_013062.1	VEGFR-2	AGAAGGAACGAGAATGCGGG	CTCTGAAAACGCGGGTCTCT
Vascular endothelial growth factor A	NM_031836.3	VEGF-A	GGAGTCTGTGCTCTGGGATTT	GTGAAGGAGCAACCTCTCCA
Platelet-derived growth factor receptor-β	NM_031525.1	PDGFR-β	GCCCTCATGTCGGAGTTGAA	GTTTCGGTGCAGGTAGTCCA
Raf-1 proto-oncogene, serine/threonine kinase	NM_012639.2	Raf-1	CAACGTCCACTCCCAATGTC	CTTCGAATTGCATCCTCAATCA
Nestin	NM_001308239.1	Nestin	CCCTTAGTCTGGAGGTGGCT	GGGTCCAGAAAGCCAAGAGA
Glyceraldehyde 3-phosphate dehydrogenase	NM_017008.4	GAPDH	TCTCTGCTCCTCCCTGTTCT	GGTAACCAGGCGTCCGATAC

Fig. 1. (A) Representative histological images of non-muscularized, partially muscularized, and fully muscularized intra-acinar arteries of 20 – 50 μm in diameter, respectively. NM, Non-muscular; PM, Partially muscular; FM, Fully muscular; EVG, elastic van Gieson; α-SMA, Alpha-smooth muscle actin. (B) Primer sequences for real-time polymerase chain reaction analysis of rat b-type brain natriuretic peptide (BNP), fibroblast growth factor receptor (FGFR)-1, vascular endothelial growth factor receptor (VEGFR)-2, vascular endothelial growth factor (VEGF)-A, platelet-derived growth factor receptor (PDGFR)-β, Raf-1 proto-oncogene serine/threonine kinase (Raf-1), nestin, and glyceraldehyde 3-phosphate dehydrogenase (GAPDH).

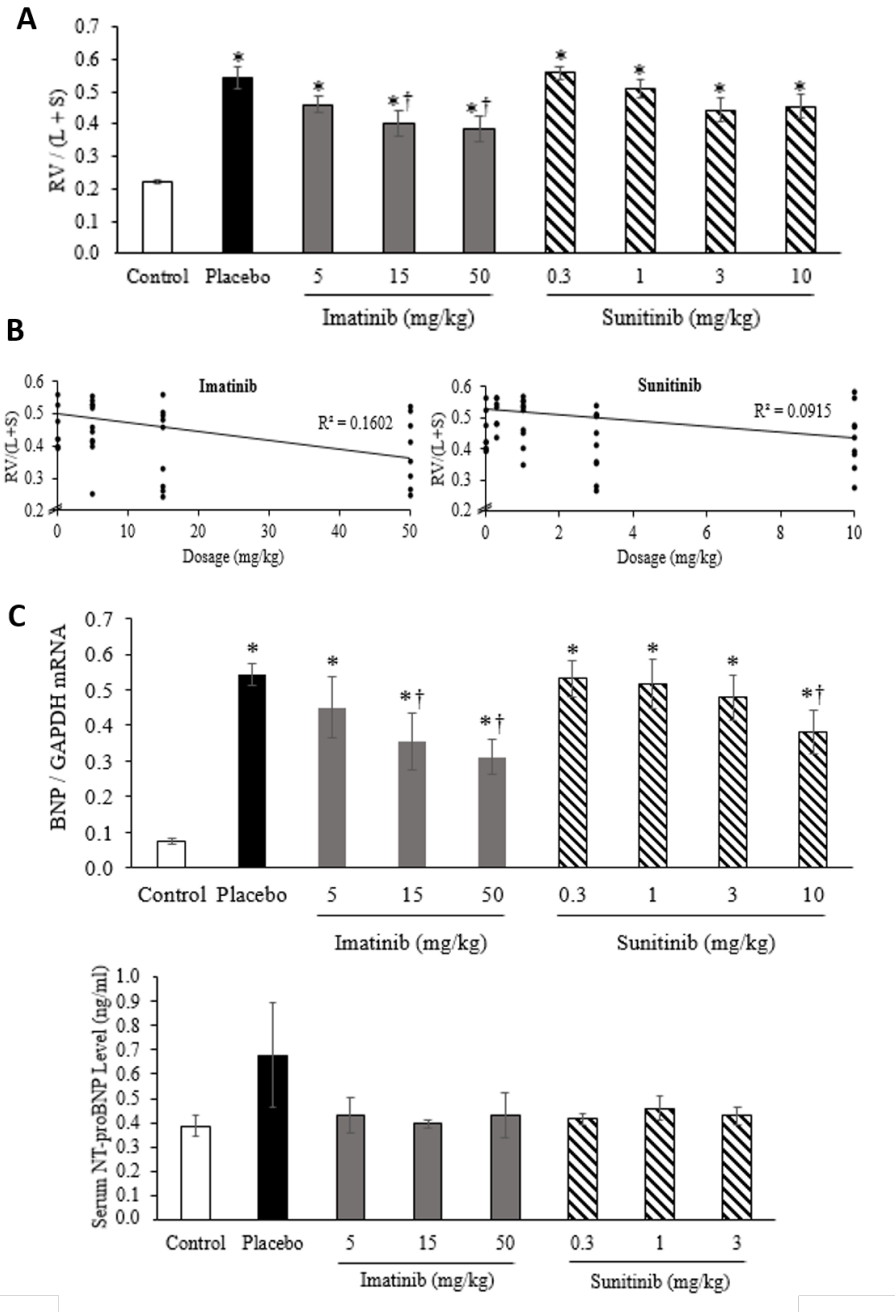

Fig. 2. Effects of imatinib and sunitinib on monocrotaline-induced right ventricular hypertrophy (RVH) and hypertrophy markers. (A) RVH of different groups. N = 8 – 14. (B) RVH reversal dose-dependency of imatinib and sunitinib. N = 8 – 14. (C) Relative brain natriuretic peptide (BNP) mRNA expression in the RV tissue. N = 8 – 14. (D) Serum level of N-terminal pro-brain natriuretic peptide (NT-proBNP). N = 5 – 6. Data are mean ± SEM. *$P < 0.05$ vs. control; $^{\dagger}P < 0.05$ vs. placebo.

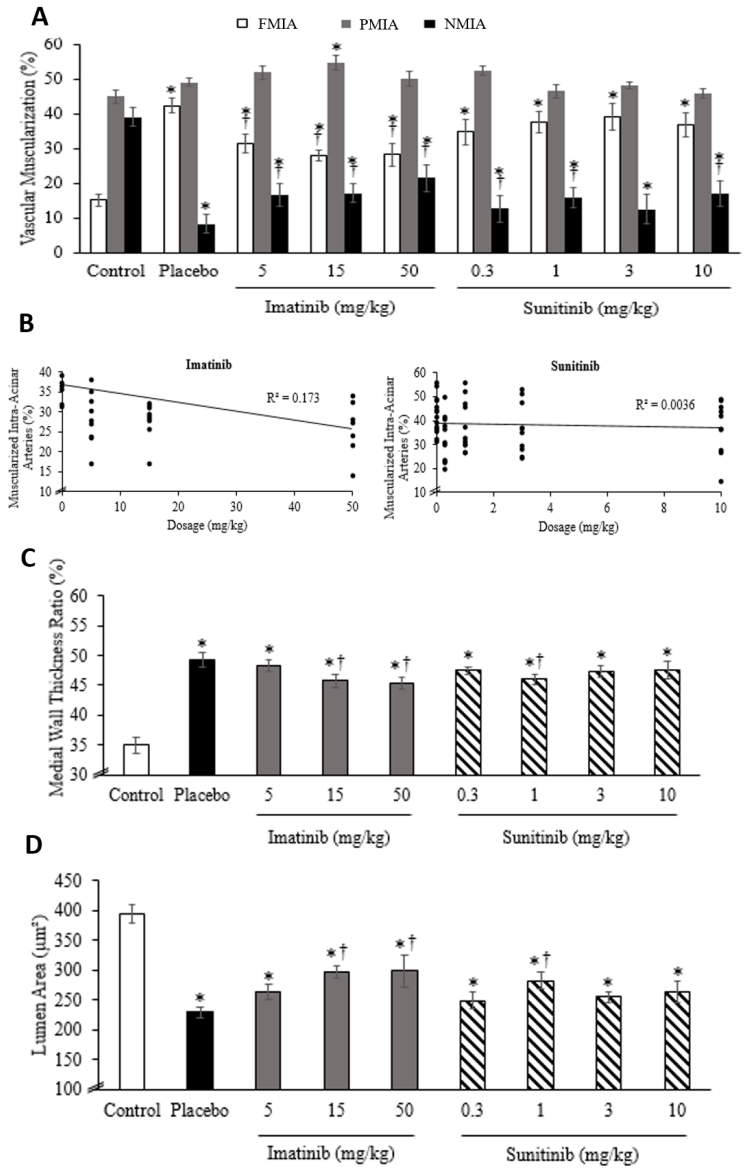

Fig. 3. Effects of imatinib and sunitinib on vascular muscularization in intra-acinar arteries of 20–50 μm in diameter. (A) Non-muscularized (NMIA), partially muscularized (PMIA), and fully muscularized (FMIA) intra-acinar artery percentage related to the total number of pulmonary arteries quantified. (B) Dose-dependency of imatinib and sunitinib on pulmonary muscularization reversal. (C) Medial wall thickness normalized to the external diameter of the fully muscularized intra-acinar arteries. (D) Lumen area of the fully muscularized intra-acinar arteries. Data are mean ± SEM (N = 8 – 14). *$P < 0.05$ vs. control; $^{\dagger}P < 0.05$ vs. placebo.

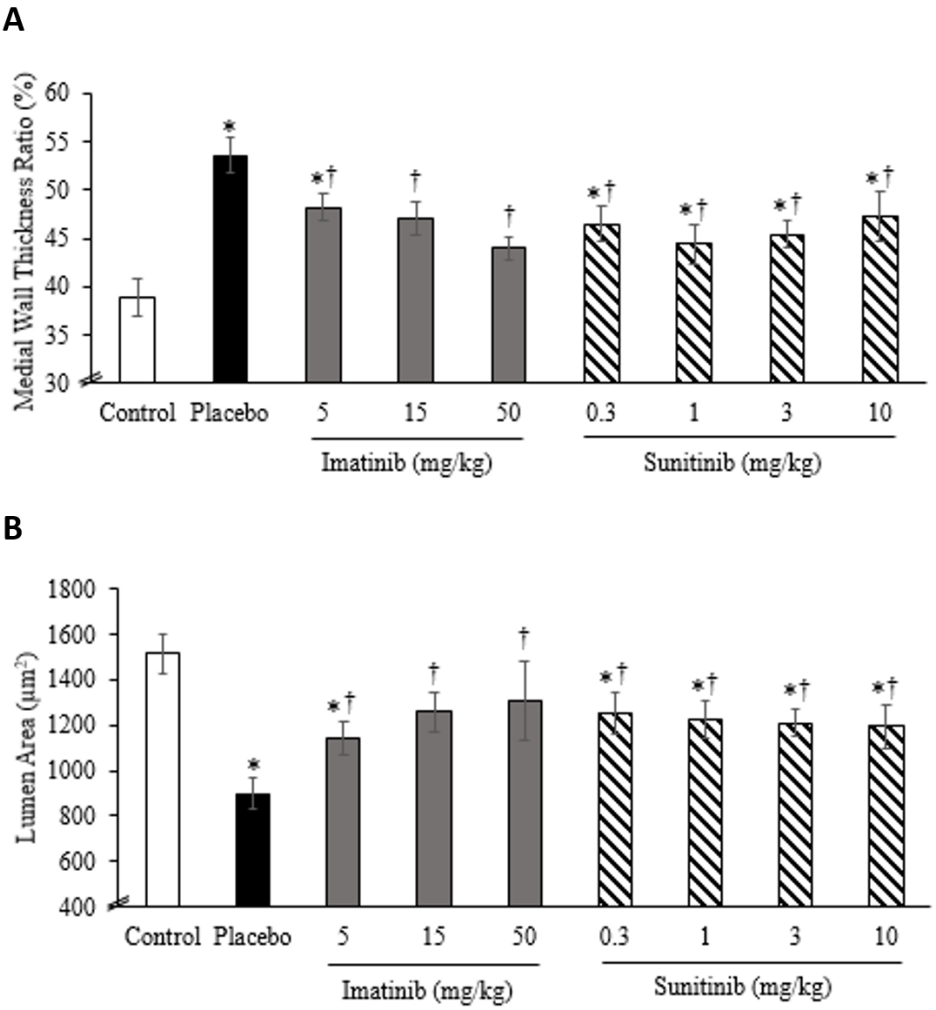

Fig. 4. Effects of imatinib and sunitinib on vascular muscularization in the intra-acinar arteries of 51–100 μm in diameter. (A) Medial wall thickness normalized to the external diameter of the fully muscularized intra-acinar arteries. (B) Lumen area of the fully muscularized intra-acinar arteries. Data are mean ± SEM (N = 8 – 14). *$P < 0.05$ vs. control; †$P < 0.05$ vs. placebo.

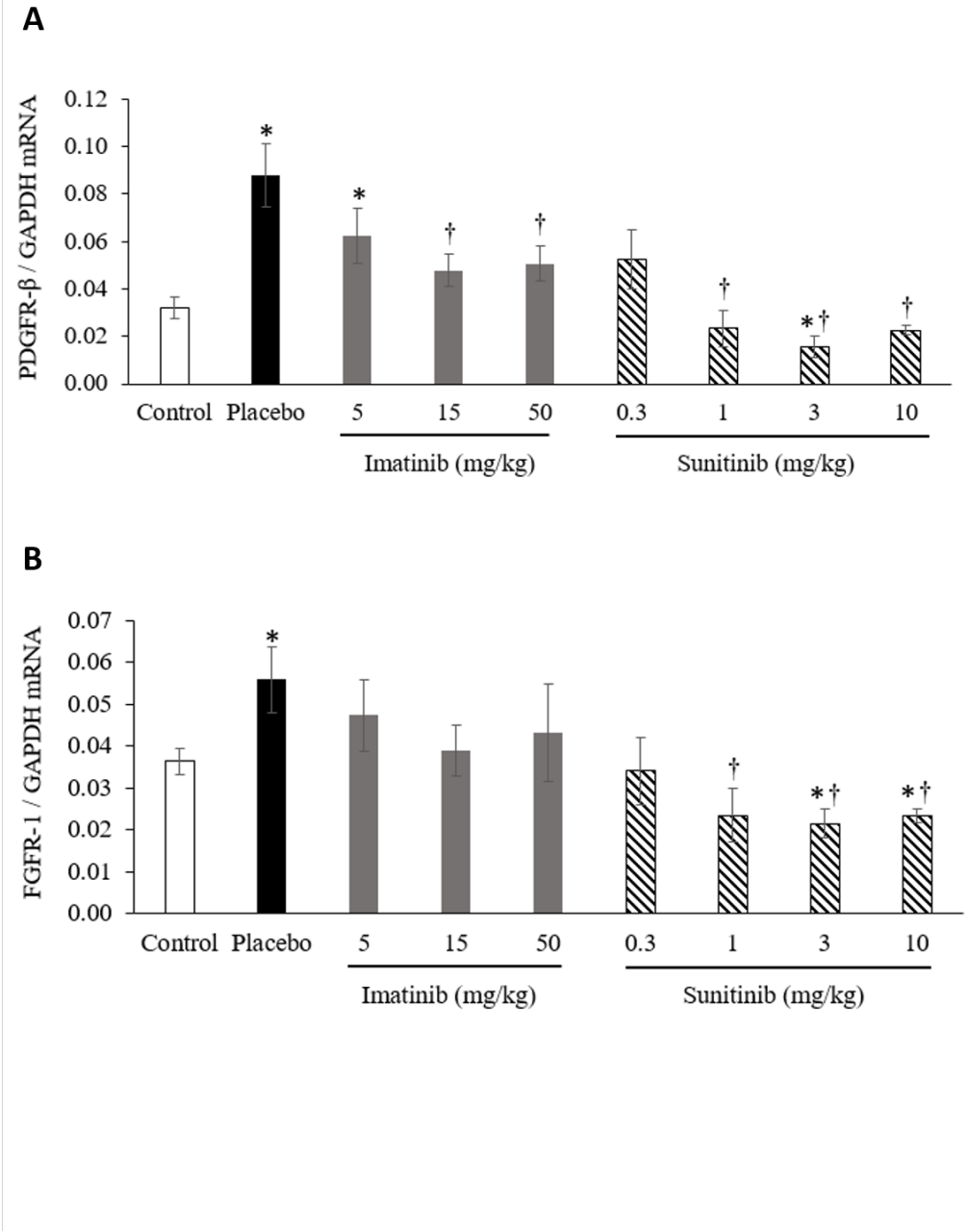

Fig. 5. Effects of imatinib and sunitinib on monocrotaline-induced receptor tyrosine kinase mRNA expression in the rat lungs. (A) Platelet-derived growth factor receptor (PDGFR)-β. N = 6 – 12. (B) Fibroblast growth factor receptor (FGFR)-1. N = 7 – 10. Data are mean ± SEM. *$P < 0.05$ vs. control; †$P < 0.05$ vs. placebo.

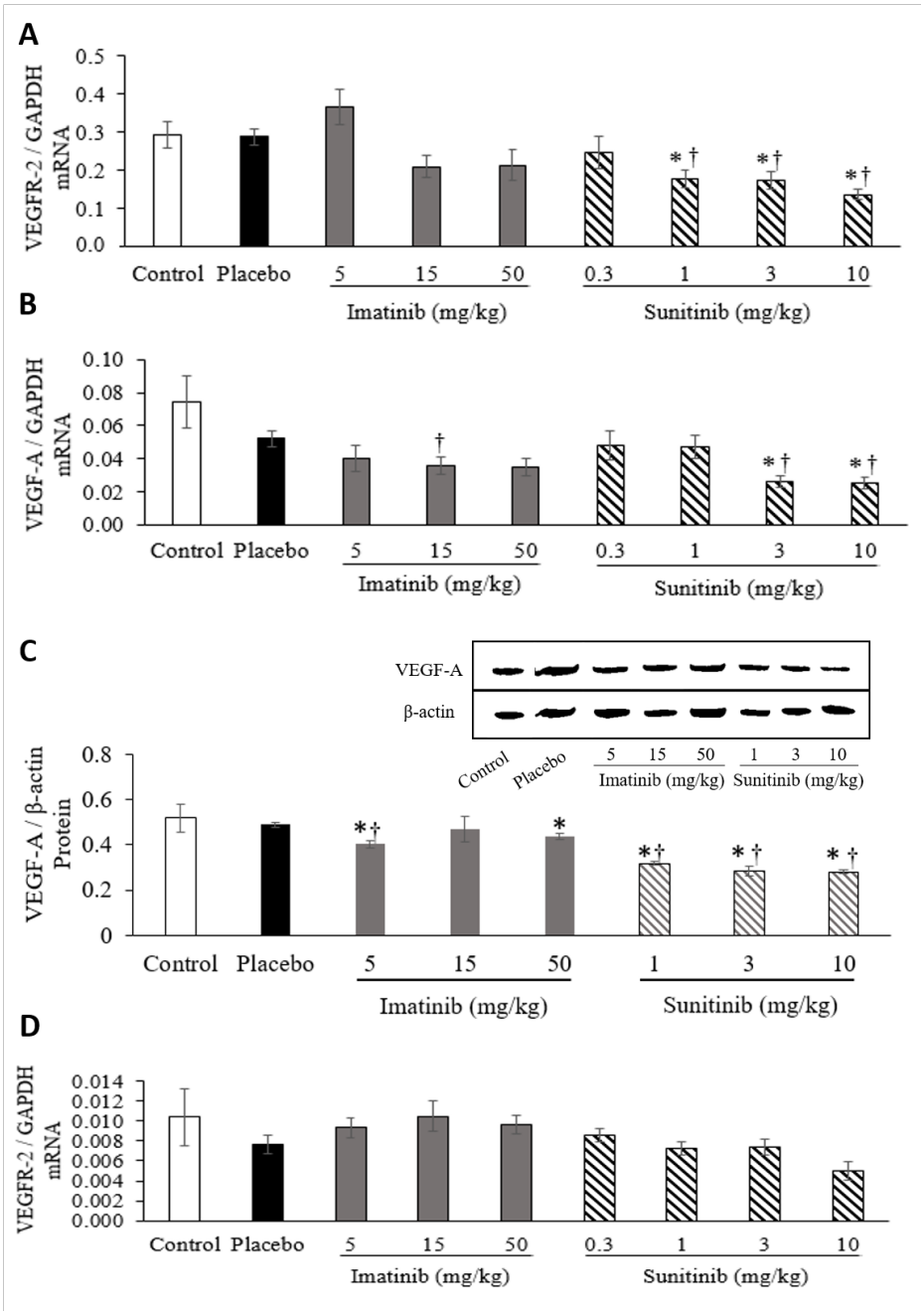

Fig. 6. Effects of imatinib and sunitinib on monocrotaline-induced vascular endothelial growth factor receptor (VEGFR)-2 mRNA expression in the rat RV and lungs, and vascular endothelial growth factor (VEGF)-A mRNA and protein expression in the rat lungs. (A) VEGFR-2 mRNA in the lungs. N = 7 – 11. (B) VEGF-A mRNA in the lungs. N = 7 – 9 (C) VEGF-A proteins in the lungs. Western blots are representative of one individual from each group. N = 3 (D) VEGFR-2 in the RV. N = 6 – 13. Data are mean ± SEM. $^{*}P < 0.05$ vs. control; $^{\dagger}P < 0.05$ vs. placebo.

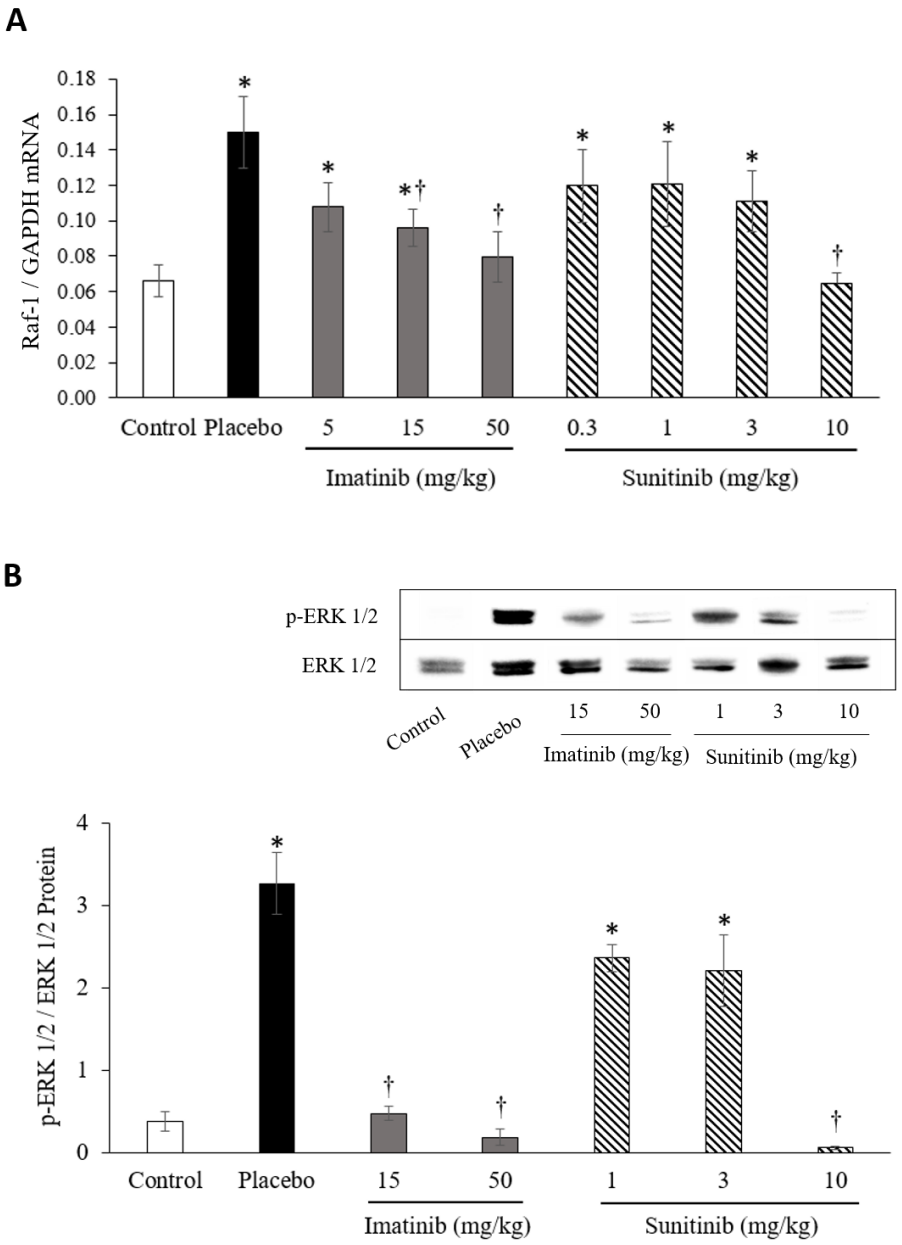

Fig. 7. Effects of imatinib and sunitinib on mitogen-activated protein kinase (MAPK) signaling pathway. (A) Raf-1 proto-oncogene serine/threonine kinase (Raf-1) mRNA expression in the lungs. N = 8 – 14. (B) Phosphorylation of extra-cellular-signal-related kinase (ERK)-1/2 protein expression in the lungs. Western blots are representative of one individual from each group. N = 3. Data are mean ± SEM. *P < 0.05 vs. control; †P < 0.05 vs. placebo.

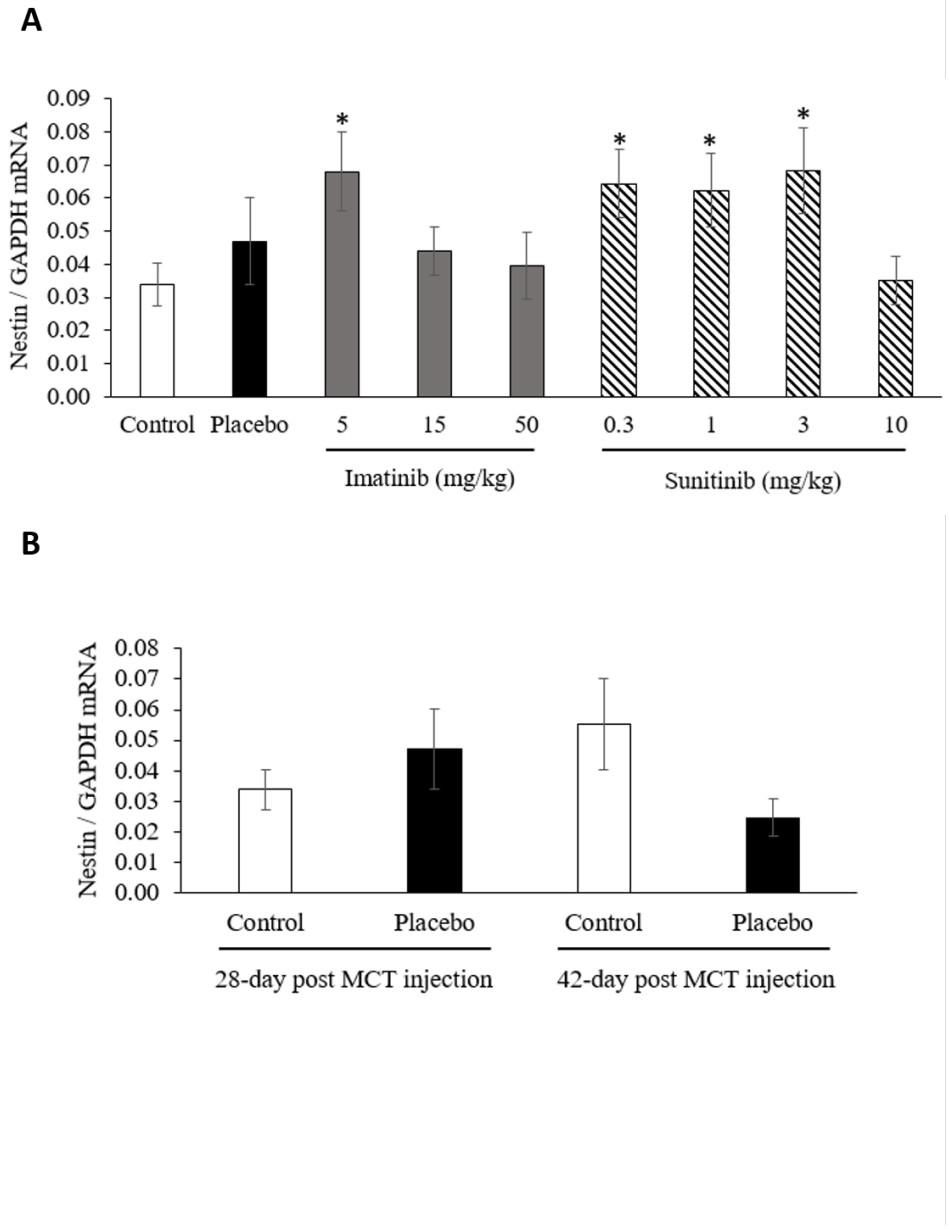

Fig. 8. Effects of imatinib and sunitinib on monocrotaline-induced angiogenesis marker nestin mRNA expression in the rat lungs. (A) Nestin mRNA expression in the different groups. N = 7 – 9. (B) The comparison of nestin mRNA expression between the control and the placebo 28 and 42 days after the MCT injection. N = 6 – 13. Data are mean ± SEM. *$P < 0.05$ vs control; $^{\dagger}P < 0.05$ vs. placebo.